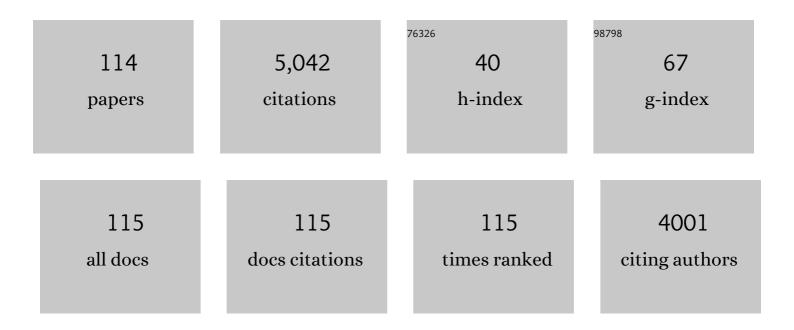


List of Publications by Year in descending order

Source: https://exaly.com/author-pdf/4391728/publications.pdf Version: 2024-02-01



K MAVED

#	Article	IF	CITATIONS
1	Reactive transport codes for subsurface environmental simulation. Computational Geosciences, 2015, 19, 445-478.	2.4	566
2	Multicomponent reactive transport modeling in variably saturated porous media using a generalized formulation for kinetically controlled reactions. Water Resources Research, 2002, 38, 13-1-13-21.	4.2	429
3	Expanding the role of reactive transport models in critical zone processes. Earth-Science Reviews, 2017, 165, 280-301.	9.1	207
4	Reactive transport modeling in fractured rock: A state-of-the-science review. Earth-Science Reviews, 2005, 72, 189-227.	9.1	164
5	Modelling the biogeochemical cycle of silicon in soils: Application to a temperate forest ecosystem. Geochimica Et Cosmochimica Acta, 2008, 72, 741-758.	3.9	156
6	Rates of sulfate reduction and metal sulfide precipitation in a permeable reactive barrier. Applied Geochemistry, 2002, 17, 301-320.	3.0	136
7	Reactive transport modeling of an in situ reactive barrier for the treatment of hexavalent chromium and trichloroethylene in groundwater. Water Resources Research, 2001, 37, 3091-3103.	4.2	132
8	Offsetting of CO2 emissions by air capture in mine tailings at the Mount Keith Nickel Mine, Western Australia: Rates, controls and prospects for carbon neutral mining. International Journal of Greenhouse Gas Control, 2014, 25, 121-140.	4.6	113
9	Mobility and persistence of methane in groundwater in a controlled-release fieldÂexperiment. Nature Geoscience, 2017, 10, 289-294.	12.9	106
10	Use of dissolved and vapor-phase gases to investigate methanogenic degradation of petroleum hydrocarbon contamination in the subsurface. Water Resources Research, 2005, 41, .	4.2	99
11	Influence of surface passivation and water content on mineral reactions in unsaturated porous media: Implications for brucite carbonation and CO2 sequestration. Geochimica Et Cosmochimica Acta, 2015, 148, 477-495.	3.9	94
12	Investigating the role of gas bubble formation and entrapment in contaminated aquifers: Reactive transport modelling. Journal of Contaminant Hydrology, 2006, 87, 123-154.	3.3	87
13	Reactive transport modeling of processes controlling the distribution and natural attenuation of phenolic compounds in a deep sandstone aquifer. Journal of Contaminant Hydrology, 2001, 53, 341-368.	3.3	86
14	Vadose zone attenuation of organic compounds at a crude oil spill site — Interactions between biogeochemical reactions and multicomponent gas transport. Journal of Contaminant Hydrology, 2010, 112, 15-29.	3.3	86
15	Modelling the closure-related geochemical evolution of groundwater at a former uranium mine. Journal of Contaminant Hydrology, 2001, 52, 109-135.	3.3	81
16	CO ₂ -Efflux Measurements for Evaluating Source Zone Natural Attenuation Rates in a Petroleum Hydrocarbon Contaminated Aquifer. Environmental Science & Technology, 2011, 45, 482-488.	10.0	69
17	Reactive Transport Modeling of Trichloroethene Treatment with Declining Reactivity of Iron. Environmental Science & Technology, 2007, 41, 1432-1438.	10.0	66
18	Reactive Transport in Evolving Porous Media. Reviews in Mineralogy and Geochemistry, 2019, 85, 197-238.	4.8	65

#	Article	IF	CITATIONS
19	Process-based reactive transport modeling of a permeable reactive barrier for the treatment of mine drainage. Journal of Contaminant Hydrology, 2006, 85, 195-211.	3.3	64
20	Modeling Kinetic Processes Controlling Hydrogen and Acetate Concentrations in an Aquifer-Derived Microcosm. Environmental Science & Technology, 2003, 37, 3910-3919.	10.0	62
21	Implementation and evaluation of permeability-porosity and tortuosity-porosity relationships linked to mineral dissolution-precipitation. Computational Geosciences, 2015, 19, 655-671.	2.4	60
22	Three-dimensional density-dependent flow and multicomponent reactive transport modeling of chlorinated solvent oxidation by potassium permanganate. Journal of Contaminant Hydrology, 2009, 106, 195-211.	3.3	57
23	Effectiveness of various cover scenarios on the rate of sulfide oxidation of mine tailings. Journal of Hydrology, 2003, 271, 171-187.	5.4	53
24	Investigating Ebullition in a Sand Column Using Dissolved Gas Analysis and Reactive Transport Modeling. Environmental Science & Technology, 2006, 40, 5361-5367.	10.0	51
25	Reactive Transport Modeling of Column Experiments for the Remediation of Acid Mine Drainage. Environmental Science & Technology, 2004, 38, 3131-3138.	10.0	50
26	Integration of field measurements and reactive transport modelling to evaluate contaminant transport at a sulfide mine tailings impoundment. Journal of Contaminant Hydrology, 2006, 88, 1-22.	3.3	50
27	Comparison of numerical methods for simulating strongly nonlinear and heterogeneous reactive transport problems—the MoMaS benchmark case. Computational Geosciences, 2010, 14, 483-502.	2.4	50
28	Transport and Reaction Processes Affecting the Attenuation of Landfill Gas in Cover Soils. Journal of Environmental Quality, 2008, 37, 459-468.	2.0	49
29	Methane emissions and contaminant degradation rates at sites affected by accidental releases of denatured fuel-grade ethanol. Journal of Contaminant Hydrology, 2013, 151, 1-15.	3.3	48
30	Acidic Microenvironments in Waste Rock Characterized by Neutral Drainage: Bacteria–Mineral Interactions at Sulfide Surfaces. Minerals (Basel, Switzerland), 2014, 4, 170-190.	2.0	47
31	Transport Implications Resulting from Internal Redistribution of Arsenic and Iron within Constructed Soil Aggregates. Environmental Science & Technology, 2011, 45, 582-588.	10.0	46
32	Long-term monitoring of waste-rock weathering at the Antamina mine, Peru. Chemosphere, 2019, 215, 858-869.	8.2	46
33	Verification and intercomparison of reactive transport codes to describe root-uptake. Plant and Soil, 2006, 285, 305-321.	3.7	45
34	Characterizing Vadose Zone Hydrocarbon Biodegradation Using Carbon Dioxide Effluxes, Isotopes, and Reactive Transport Modeling. Vadose Zone Journal, 2012, 11, vzj2011.0204.	2.2	45
35	Benchmark reactive transport simulations of a column experiment in compacted bentonite with multispecies diffusion and explicit treatment of electrostatic effects. Computational Geosciences, 2015, 19, 535-550.	2.4	45
36	Molybdenum and zinc stable isotope variation in mining waste rock drainage and waste rock at the Antamina mine, Peru. Science of the Total Environment, 2016, 550, 103-113.	8.0	44

#	Article	IF	CITATIONS
37	Solution of the MoMaS reactive transport benchmark with MIN3P—model formulation and simulation results. Computational Geosciences, 2010, 14, 405-419.	2.4	43
38	Benchmarks for multicomponent reactive transport across a cement/clay interface. Computational Geosciences, 2015, 19, 635-653.	2.4	43
39	The impact of evolving mineral–water–gas interfacial areas on mineral–fluid reaction rates in unsaturated porous media. Chemical Geology, 2016, 421, 65-80.	3.3	43
40	Barometric-pumping controls fugitive gas emissions from a vadose zone natural gas release. Scientific Reports, 2019, 9, 14080.	3.3	43
41	Benchmarks for multicomponent diffusion and electrochemical migration. Computational Geosciences, 2015, 19, 523-533.	2.4	42
42	Microbial and geochemical controls on waste rock weathering and drainage quality. Science of the Total Environment, 2018, 640-641, 1004-1014.	8.0	37
43	Identification, spatial extent and distribution of fugitive gas migration on the well pad scale. Science of the Total Environment, 2019, 652, 356-366.	8.0	37
44	A detailed field-based evaluation of naphthenic acid mobility in groundwater. Journal of Contaminant Hydrology, 2009, 108, 89-106.	3.3	36
45	Can argillaceous formations isolate nuclear waste? Insights from isotopic, noble gas, and geochemical profiles. Geofluids, 2015, 15, 381-386.	0.7	36
46	Multicomponent reactive transport modeling of acid neutralization reactions in mine tailings. Water Resources Research, 2004, 40, .	4.2	34
47	High resolution spatial and temporal evolution of dissolved gases in groundwater during a controlled natural gas release experiment. Science of the Total Environment, 2018, 622-623, 1178-1192.	8.0	33
48	Changes in mineral reactivity driven by pore fluid mobility in partially wetted porous media. Chemical Geology, 2017, 463, 1-11.	3.3	32
49	Advancing knowledge of gas migration and fugitive gas from energy wells in northeast British Columbia, Canada. , 2019, 9, 134-151.		32
50	Reactive transport benchmarks for subsurface environmental simulation. Computational Geosciences, 2015, 19, 439-443.	2.4	31
51	Identification of key parameters controlling dissolved oxygen migration and attenuation in fractured crystalline rocks. Journal of Contaminant Hydrology, 2008, 95, 141-153.	3.3	30
52	Comparison of unsaturated flow and solute transport through waste rock at two experimental scales using temporal moments and numerical modeling. Journal of Contaminant Hydrology, 2014, 171, 49-65.	3.3	28
53	Parallelization of MIN3P-THCm: A high performance computational framework for subsurface flow and reactive transport simulation. Environmental Modelling and Software, 2017, 95, 271-289.	4.5	28
54	Hydro-biogeochemical impacts of fugitive methane on a shallow unconfined aquifer. Science of the Total Environment, 2019, 690, 1342-1354.	8.0	28

#	Article	IF	CITATIONS
55	Aggregateâ€6cale Heterogeneity in Iron (Hydr)oxide Reductive Transformations. Vadose Zone Journal, 2009, 8, 1004-1012.	2.2	26
56	Benchmark problems for reactive transport modeling of the generation and attenuation of acid rock drainage. Computational Geosciences, 2015, 19, 599-611.	2.4	26
57	Solubility controls for molybdenum in neutral rock drainage. Geochemistry: Exploration, Environment, Analysis, 2012, 12, 21-32.	0.9	24
58	Evaluation of Seasonal Factors on Petroleum Hydrocarbon Vapor Biodegradation and Intrusion Potential in a Cold Climate. Ground Water Monitoring and Remediation, 2014, 34, 60-78.	0.8	23
59	Stochastic multicomponent reactive transport analysis of low quality drainage release from waste rock piles: Controls of the spatial distribution of acid generating and neutralizing minerals. Journal of Contaminant Hydrology, 2017, 201, 30-38.	3.3	23
60	Tracing Molybdenum Attenuation in Mining Environments Using Molybdenum Stable Isotopes. Environmental Science & Technology, 2019, 53, 5678-5686.	10.0	23
61	Mobilization of Metal(oid) Oxyanions through Circumneutral Mine Waste-Rock Drainage. ACS Omega, 2019, 4, 10205-10215.	3.5	22
62	MIN3P-HPC: A High-Performance Unstructured Grid Code for Subsurface Flow and Reactive Transport Simulation. Mathematical Geosciences, 2021, 53, 517-550.	2.4	22
63	Manganese Valence in Oxides Formed from in Situ Chemical Oxidation of TCE by KMnO ₄ . Environmental Science & Technology, 2010, 44, 5934-5939.	10.0	21
64	Evaluation of single- and dual-porosity models for reproducing the release of external and internal tracers from heterogeneous waste-rock piles. Journal of Contaminant Hydrology, 2018, 214, 65-74.	3.3	19
65	Metal mobility during in situ chemical oxidation of TCE by KMnO4. Journal of Contaminant Hydrology, 2006, 88, 137-152.	3.3	18
66	Spatial and Temporal Fluctuations of Poreâ€Gas Composition in Sulfidic Mine Waste Rock. Vadose Zone Journal, 2016, 15, 1-13.	2.2	18
67	Determination of mineral dissolution regimes using flow-through time-resolved analysis (FT-TRA) and numerical simulation. Chemical Geology, 2016, 430, 1-12.	3.3	18
68	Localized Sulfide Oxidation Limited by Oxygen Supply in a Full‣cale Wasteâ€Rock Pile. Vadose Zone Journal, 2018, 17, 1-14.	2.2	18
69	Biogeochemical processes controlling the mobility of major ions and trace metals in aquitard sediments beneath an oil sand tailing pond: Laboratory studies and reactive transport modeling. Journal of Contaminant Hydrology, 2013, 151, 55-67.	3.3	17
70	The importance of conceptual models in the reactive transport simulation of oxygen ingress in sparsely fractured crystalline rock. Journal of Contaminant Hydrology, 2010, 112, 64-76.	3.3	16
71	Scale dependence of effective geochemical rates in weathering mine waste rock. Journal of Contaminant Hydrology, 2020, 234, 103699.	3.3	16
72	Electrical Monitoring of In Situ Chemical Oxidation by Permanganate. Ground Water Monitoring and Remediation, 2007, 27, 77-84.	0.8	15

#	Article	IF	CITATIONS
73	Diel plant water use and competitive soil cation exchange interact to enhance NH4 + and K+ availability in the rhizosphere. Plant and Soil, 2017, 414, 33-51.	3.7	15
74	Laboratory-scale experimental and modelling investigations of 222Rn profiles in chemically heterogeneous LNAPL contaminated vadose zones. Science of the Total Environment, 2019, 681, 456-466.	8.0	15
75	Impacts of water table fluctuations on actual and perceived natural source zone depletion rates. Journal of Contaminant Hydrology, 2021, 238, 103771.	3.3	15
76	A study of Zn and Mo attenuation by waste-rock mixing in neutral mine drainage using mixed-material field barrels and humidity cells. Applied Geochemistry, 2017, 84, 114-125.	3.0	14
77	Manganese and trace-metal mobility under reducing conditions following in situ oxidation of TCE by KMnO4: A laboratory column experiment. Journal of Contaminant Hydrology, 2011, 119, 13-24.	3.3	13
78	Atmospheric noble gases as tracers of biogenic gas dynamics in a shallow unconfined aquifer. Geochimica Et Cosmochimica Acta, 2014, 128, 144-157.	3.9	13
79	Decalcification of cracked cement structures. Computational Geosciences, 2015, 19, 673-693.	2.4	13
80	Mineralogical controls on drainage quality during the weathering of waste rock. Applied Geochemistry, 2019, 108, 104376.	3.0	13
81	Poregas distributions in waste-rock piles affected by climate seasonality and physicochemical heterogeneity. Applied Geochemistry, 2019, 100, 305-315.	3.0	13
82	Geochemical and mineralogical assessment of reactivity in a full-scale heterogeneous waste-rock pile. Minerals Engineering, 2020, 145, 106089.	4.3	13
83	Release of geogenic uranium and arsenic results in water-quality impacts in a subarctic permafrost region of granitic and metamorphic geology. Journal of Geochemical Exploration, 2020, 217, 106607.	3.2	13
84	Modeling Vadose Zone Processes during Land Application of Foodâ€Processing Waste Water in California's Central Valley. Journal of Environmental Quality, 2008, 37, S43-57.	2.0	12
85	Determination of spatially-resolved porosity, tracer distributions and diffusion coefficients in porous media using MRI measurements and numerical simulations. Journal of Contaminant Hydrology, 2011, 125, 47-56.	3.3	12
86	Using noble gas tracers to constrain a groundwater flow model with recharge elevations: A novel approach for mountainous terrain. Water Resources Research, 2015, 51, 8094-8113.	4.2	12
87	Measuring mineral dissolution kinetics using on-line flow-through time resolved analysis (FT-TRA): an exploratory study with forsterite. Chemical Geology, 2015, 413, 107-118.	3.3	12
88	The Art of Reactive Transport Model Building. Elements, 2019, 15, 117-118.	0.5	12
89	Numerical Modeling of a Laboratory-Scale Waste Rock Pile Featuring an Engineered Cover System. Minerals (Basel, Switzerland), 2020, 10, 652.	2.0	12
90	Spatiotemporal variability of fugitive gas migration emissions around a petroleum well. Atmospheric Pollution Research, 2021, 12, 101094.	3.8	12

#	Article	IF	CITATIONS
91	Evaluating methods for quantifying cation exchange in mildly calcareous sediments in Northern Alberta. Applied Geochemistry, 2012, 27, 2511-2523.	3.0	11
92	Unintentional contaminant transfer from groundwater to the vadose zone during source zone remediation of volatile organic compounds. Journal of Contaminant Hydrology, 2017, 204, 1-10.	3.3	11
93	Diffusion–reaction studies in low permeability shale using X-ray radiography with cesium. Applied Geochemistry, 2013, 39, 49-58.	3.0	10
94	A benchmark for microbially mediated chromium reduction under denitrifying conditions in a biostimulation column experiment. Computational Geosciences, 2015, 19, 479-496.	2.4	10
95	Tracking Diverse Minerals, Hungry Organisms, and Dangerous Contaminants Using Reactive Transport Models. Elements, 2019, 15, 81-86.	0.5	10
96	Numerical investigation of flow instabilities using fully unstructured discretization for variably saturated flow problems. Advances in Water Resources, 2020, 143, 103673.	3.8	10
97	A benchmark for multi-rate surface complexation and 1D dual-domain multi-component reactive transport of U(VI). Computational Geosciences, 2015, 19, 585-597.	2.4	8
98	Reactive Transport of Manureâ€Derived Nitrogen in the Vadose Zone: Consideration of Macropore Connectivity to Subsurface Receptors. Vadose Zone Journal, 2019, 18, 1-18.	2.2	8
99	Geochemical Controls on Uranium Release from Neutral-pH Rock Drainage Produced by Weathering of Granite, Gneiss, and Schist. Minerals (Basel, Switzerland), 2020, 10, 1104.	2.0	8
100	Controls of uncertainty in acid rock drainage predictions from waste rock piles examined through Monte-Carlo multicomponent reactive transport. Stochastic Environmental Research and Risk Assessment, 2020, 34, 219-233.	4.0	7
101	Modeling of Thermal-Hydrological-Chemical (THC) Processes During Waste Rock Weathering Under Permafrost Conditions. Frontiers in Water, 2021, 3, .	2.3	7
102	Thermal-Hydrological-Chemical Modeling of a Covered Waste Rock Pile in a Permafrost Region. Minerals (Basel, Switzerland), 2021, 11, 565.	2.0	7
103	Investigating the Influence of Structure and Heterogeneity in Waste Rock Piles on Mass Loading Rates—A Reactive Transport Modeling Study. Frontiers in Water, 2021, 3, .	2.3	7
104	Persistence of Uranium in Old and Cold Subpermafrost Groundwater Indicated by Linking ²³⁴ U- ²³⁵ U- ²³⁸ U, Groundwater Ages, and Hydrogeochemistry. ACS Earth and Space Chemistry, 2021, 5, 3474-3487.	2.7	6
105	Reactive transport modeling of 90Sr sorption in reactive sandpacks. Journal of Hazardous Materials, 2014, 280, 685-695.	12.4	5
106	A reactive transport benchmark on modeling biogenic uraninite re-oxidation by Fe(III)-(hydr)oxides. Computational Geosciences, 2015, 19, 569-583.	2.4	5
107	Evaluation of the Potential for Dissolved Oxygen Ingress into Deep Sedimentary Basins during a Glaciation Event. Geofluids, 2018, 2018, 1-20.	0.7	5
108	Towards quantifying subsurface methane emissions from energy wells with integrity failure. Atmospheric Pollution Research, 2021, 12, 101223.	3.8	5

#	Article	IF	CITATIONS
109	Quantifying natural source zone depletion at petroleum hydrocarbon contaminated sites: A comparison of 14C methods. Journal of Contaminant Hydrology, 2021, 240, 103795.	3.3	4
110	Reactive transport modelling the oxalate-carbonate pathway of the Iroko tree; Investigation of calcium and carbon sinks and sources. Geoderma, 2022, 410, 115665.	5.1	4
111	Travel time-based modelling of nitrate reduction in a fractured limestone aquifer by pyrite and iron carbonates under pore size limitation. Journal of Contaminant Hydrology, 2022, 248, 103983.	3.3	2
112	Reactive transport investigations of the long-term geochemical evolution of a multibarrier system including bentonite, low-alkali concrete and host rock. Applied Geochemistry, 2022, 143, 105385.	3.0	2
113	7. Reactive Transport in Evolving Porous Media. , 2019, , 197-238.		1
114	The nature of gas production patterns associated with methanol degradation in natural aquifer sediments: A microcosm study. Journal of Contaminant Hydrology, 2022, 247, 103988.	3.3	0